

## Diffusion and Sorption of Nitroplasticizers in Vinyl Copolymer Elastomer and Its Composites

Dali Yang, Robin Pacheco, Kevin Henderson, Kevin Hubbard, David Devlin

Polymers and Coatings Group, Materials Science and Technology Division, Los Alamos National Laboratory, Los Alamos, New Mexico, 87545

Correspondence to: D. Yang (E-mail: dyang@lanl.gov)

**ABSTRACT:** To study the aging behavior of cured vinyl copolymer elastomer (VCE) under thermal and nitroplasticizer (NP) environment, we investigated the sorption and diffusion of NP in VCE and its composites. The sorption kinetics of NP into VCE and its composites with respect to filler concentration (0–80%) and temperature (18–70°C) were investigated by conventional gravimetric method. The NP sorption process is endothermic. Kinetic studies show that Fickian diffusion can describe the NP sorption in the VCE polymer. The samples with a high filler concentration show more complicated behavior at low temperature than that at high temperature. The present article discusses the dependences of diffusion coefficient and other related parameters on the polymer concentration and morphological structures of the samples. © 2014 Wiley Periodicals, Inc. *J. Appl. Polym. Sci.* **2014**, *131*, 40729.

**KEYWORDS:** adsorption; composites; elastomers; morphology; plasticizer

Received 22 January 2014; accepted 17 March 2014

DOI: 10.1002/app.40729

### INTRODUCTION

Vinyl copolymer elastomer is an ethylene/vinyl acetate/vinyl alcohol terpolymer. It is commonly used as a binder for highly filled elastomeric materials.<sup>1–3</sup> Because of its wide use, it is important to ascertain possible risks associated with aging. When stored in application systems, VCE slowly uptakes nitroplasticizers (NP) from the surroundings. As NP uptake progresses, NP may change the thermal and mechanical properties of VCE. Despite the previous studies,<sup>1–7</sup> the knowledge of VCE aging under NP environment is limited. Therefore, it is critical to know how plasticizer content, temperature, aging and/or a combination of these factors affect the properties of VCE. This article is the first of a series on VCE, with the objective of understanding the NP uptake, adhesion, and aging behavior of VCE and developing models to reliably predict useful service life under a wide variety of storage conditions.

VCEs have been produced at Honeywell's Kansas City Plant (KCP) for many years. The manufacturing process involves the controlled hydrolysis of ethylene vinyl acetate (EVA) to give the ethylene/vinyl acetate/vinyl alcohol terpolymer (uncured VCE), as shown in Figure 1. The requirement for the hydroxyl content ( $z$ ) in VCE is 1.0–2.0%. A cured VCE is cross-linked using diphenyl-4,4'-methylenebis(phenylcarbamate) (Hylene MP). The uncured VCE and Hylene MP are compounded together.<sup>2</sup> The chemistry of curing process to produce the cured VCE is depicted in Figure 2. The cured VCE (herein simply called

VCE) is what is commonly used for most applications and will be studied in this work. For filled VCEs, filler particles are added during the compounding process. The VCEs containing filler particles are referred to as VCE composites.

Although a plasticizer can be inert or energetic, the energetic one is often used to increase the compatibility between explosive powder and inert binders in addition to lowering the sensitivity of the explosive and improving the processibility (e.g., increasing its flexibility and tensile strength)<sup>8,9</sup> Generally, the energetic plasticizers contain nitro and/or nitrate compounds (referred to as nitroplasticizers). One nitroplasticizer that has found widespread use in energetic formulations is an eutectic mixture of bis(2,2-dinitropropyl)acetal and formal (BDNPA/F) (herein also referred to as NP). Its molecular structure is shown in Figure 3. In the BDNPA/F form, its boiling point, melting point and density are 150°C, –15°C, and 1.383–1.397 g cm<sup>-3</sup>, respectively.<sup>10</sup> NP is commonly used in polymer-bonded explosive (PBX) and gun propellant formulations.<sup>11–14</sup> One problem with the plasticizers is that they are generally low molecular weight chemicals and have a tendency to migrate from one material to another. The migration of plasticizer has been reported by a number of research groups.<sup>15–17</sup> A report written in 1997 brought attention to the presence of various constituents of PBX that were being found in neighboring polymer composites, including VCE, that had been removed from the stockpile.<sup>17</sup> The study found that polymeric parts, which had

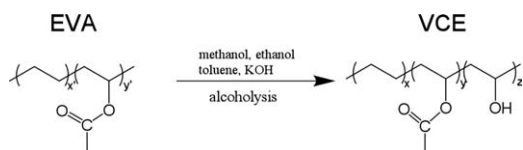


**Figure 1.** The synthesis of VCE through EVA hydrolysis ( $x = \sim 55.5\%$ ,  $y = \sim 43.0\%$ , and  $z = 1.0\text{--}2.0\%$ ).

been in the field from 100 to 188 months, contained approximately 5–6 wt % NP. Later, Fletcher et al. conducted more systematic studies to investigate the effect of temperature and NP source configuration on the NP uptake in the VCE composites. At the end of 300-day study, they found that the NP concentration in the VCE was as high as 8 wt %, and did not reach a plateau yet.<sup>18</sup> The maximum NP uptake is not clear. The affinity between VCE and NP molecules can be attributed to the carbonyl oxygen at both ester and urethane links in VCE and to the polar nitro and ether groups in NP, which can form hydrogen bonds readily. Although the depletion of NP seems not to affect the performance of energetic materials, the NP uptake changes the mechanical and thermal properties of the VCE composites.<sup>7</sup> Therefore, it is important to understand the mass transport properties of NP sorption in the VCE and VCE composites. The objective of this research is to investigate the sorption kinetics of NP into the VCE and its composites at varying temperatures and polymer concentrations, and to develop an understanding of the controlling sorption pathways (e.g., chemisorption versus physisorption) and the mechanisms (e.g., surface sorption versus diffusion).

## EXPERIMENTAL

### Materials

The cured VCE polymer and its composites with different VCE concentrations were prepared at KCP. Un-cured VCE, cross-linker, and filler were milled together and then compressed into a flat sheet at 120°C under high pressure. The temperature was then increased to >170°C to cure the sheets for >30 min. After being cooled, the part was removed. The sheet was further post cured for a few hours at the elevated temperature to ensure out-gassing of the curing agent. Five VCE composites with different VCE concentrations (20, 30, 50, 75, and 90%) were made. NP was taken from a large lot of NP that was stored at the Pantex plant in Amarillo, TX. It is tested periodically and is staying within specifications. It contains about 0.1% of phenyl- $\beta$ -naphthylamine (PBNA, aka Neozone D) as a stabilizer. The LANL high explosives group has obtained a portion from Pantex and has stored it at room temperature. All materials were used in as-received condition.

### Gravimetric Sorption and Diffusion Measurement

Gravimetric sorption is a simple and accurate method and thus is one of the most widely used methods for the study of sorption of liquid in solid materials. It consists of following the evolution of the mass of a sample immersed in the solution. This technique is suitable for slow diffusing compounds and for the study of the initial stage of diffusion.<sup>19–22</sup>

Thin films (<1 mm) of VCE and its composites were cut into circles (diameter of 20–40 mm) by means of a sharp edged steel

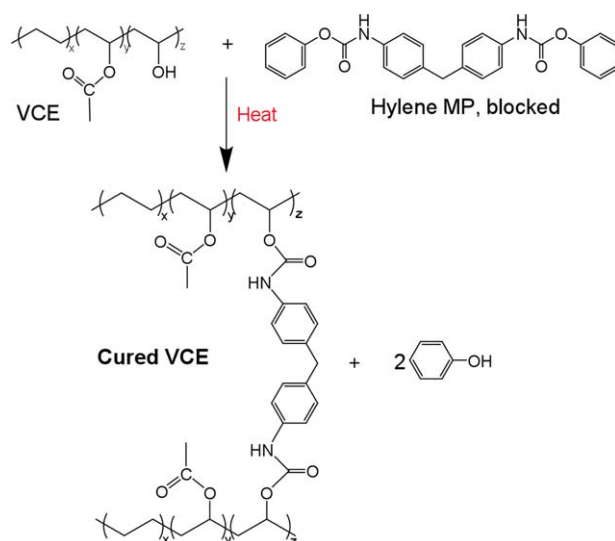


**Figure 2.** Synthesis of cured VCE by using diphenol-4,4'-methylenebis(phenylcarbamate) as a curing agent. [Color figure can be viewed in the online issue, which is available at [wileyonlinelibrary.com](http://wileyonlinelibrary.com).]

die. All samples were completely wetted and immersed inside NP, and gradually removed over the experimental course. The final samples were removed only when their max NP uptake was reached (the weight almost did not change). After the removal, the liquid NP drops adhering to the surface were wiped off using kimiwipes and the samples were weighed immediately on a digital balance (Mettler Toledo analytic balance model AL104) with accuracy  $\pm 0.01$  mg. Typically, two to three replicates were prepared. The thickness of the samples was measured before and after the immersion using a digital caliper with accuracy  $\pm 0.01$  mm. The sorption experiments were conducted at 18–22, 38, 55, and 70°C. To ensure thermal equilibrium of the NP liquid and samples, the NP containers and the VCE samples were separately preheated to the desired temperature in regulated ovens for  $\sim 30$  min. This was followed by placing VCE samples into the NP containers, which were then returned to the ovens. An OMEGA MDSSi8 series meter was used to calibrate the oven temperature with an accuracy of  $\pm 1.0^\circ\text{C}$  for 38°C and  $\pm 1.5^\circ\text{C}$  for the 55 and 70°C. Since the vapor pressure of NP in this temperature range is very low,<sup>10</sup> the weight loss of NP during the sample handling is negligible. Some experimental error (<3%) results come from the immersion time lost due to the sample removal procedure.

### Thermal Analysis

A Thermal Instruments Q500 Thermogravimetric Analyzer (TGA) was used to analyze the thermal stability of NP and VCE samples. The samples were heated from ambient temperature to 600°C at  $5^\circ\text{C min}^{-1}$  with a nitrogen purge ( $10\text{ mL min}^{-1}$ ). Platinum pans were used in the TGA measurement. Differential

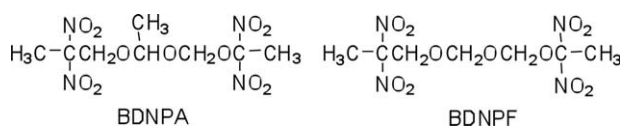


**Figure 3.** Molecular structures of nitroplasticizer (NP) (BDNPA/F).

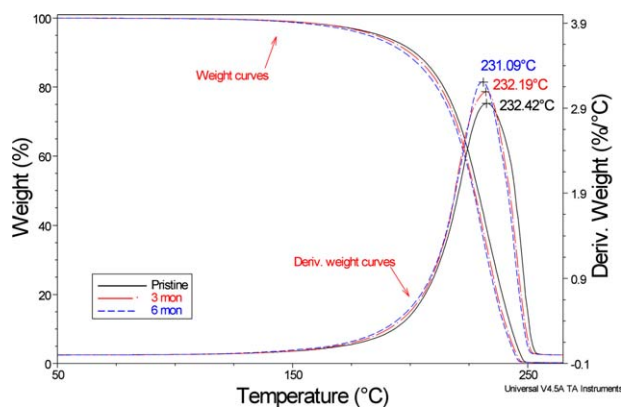


**Figure 4.** Effect of aging time on TGA results of liquid NP before and after being aged at 70°C and air environment. [Color figure can be viewed in the online issue, which is available at [wileyonlinelibrary.com](http://wileyonlinelibrary.com).]

scanning calorimetry (DSC) was carried out using a TA Instruments Q2000 Modulated Differential Scanning Calorimeter from  $-85$  to  $140^{\circ}\text{C}$  with a  $10^{\circ}\text{C min}^{-1}$  heating rate. The temperature was controlled using a refrigerated cooling accessory (RCA90). A nitrogen purge flow rate was  $50\text{ mL min}^{-1}$ . The samples were encapsulated in aluminum Tzero® pans. The instrument was calibrated with indium and sapphire standards.

#### FTIR Characterization

FTIR absorption data were obtained with a Nicolet 6700 FTIR bench operating in Attenuated Total Reflectance (ATR) mode. Specifically, the sample was held in intimate contact with a germanium crystal installed in a Spectra-Tech Thunderdome accessory. All data were taken with a resolution of  $4\text{ cm}^{-1}$ , and represent the average of 120 scans.

## RESULTS AND DISCUSSION

Before we conducted the sorption experiments, we evaluated the thermal stability of the VCE, VCE composites, and NP, and ensured that the sorption experiments were carried out under the conditions without any potential chemical degradation.

#### Thermal Properties and Stabilities of NP, VCE, and VCE Composites

Figure 4 displays the TGA results of NP before and after aging at  $70^{\circ}\text{C}$  for different times under dry air environment. The pristine NP decomposes around  $230^{\circ}\text{C}$ . After 6 month aging, this decomposition temperature slightly drops, which suggests that liquid NP is stable under dry air environment for more than a few months at  $70^{\circ}\text{C}$ . The observation is consistent with M. Finger's work.<sup>23,24</sup> Since most of the sorption experiments were finished within 20 days and below  $70^{\circ}\text{C}$ , it is reasonable to assume that the liquid NP degradation is negligible in this study.

Figure 5 presents the TGA results of a set of VCE and five composites. The VCE polymer shows two decomposition temperatures (DTemps). The first one (at  $\sim 355^{\circ}\text{C}$ ) is associated with the acetate group decomposition from its backbone while the second one (at  $\sim 4521^{\circ}\text{C}$ ) is due to the thermal decomposition of all hydrocarbon functional groups. At temperature above  $500^{\circ}\text{C}$ , VCE completely decomposes with the total weight loss of  $\sim 98.80\%$ . The results also suggest that the presence of the filler

does not change the thermal properties of the VCE polymer. For the filler, TGA result (not shown here) shows no weight loss up to  $>500^{\circ}\text{C}$ . Therefore, based on the weight loss of the VCE composites, we calculate the polymer concentration in the composites, and summarize them in Table I. For simplicity of the discussion, we label them as 20, 30, 50, 75, and 90% VCE composites.

Figure 6 presents the TGA results of the 20% VCE composites before and after being aged at different temperatures for 6 months. The results suggest that the VCEs are stable even though they were aged under the air environment at  $90^{\circ}\text{C}$  for 6 months. These results are consistent with literature.<sup>25</sup> A small peak at  $\sim 140^{\circ}\text{C}$  in the trace of the weight loss derivative in the pristine sample (also seen in Figure 5) is due to the loss of unreacted cross-linker. However, this agent is not detectable in the aged samples, suggesting that it might react with polymers over the aging process and make polymer more cross-linked. This may explain why the aged samples give slightly lower total weight loss compared with the pristine samples.

Our next consideration is the stability of VCE when it is immersed inside liquid NP at elevated temperatures. Figure 7 presents the TGA results of the VCE and its composites before and after the NP saturation. The DTemps of VCE polymer do not change for all samples. On the other hand, the DTemp of NP decreases as the filler concentration increases, which suggests that the NP becomes less stable in the VCE composites. More fundamental studies on this topic have been conducted and will be discussed in a separated paper. Here, we will focus on the NP sorption study. To avoid the complication of possible degradation of NP and VCE, all sorption experiments were conducted below  $70^{\circ}\text{C}$ . The entire sorption experiments were finished within 20 days except for the experiments conducted near the room temperature.

Figures 8(a,b) present FTIR results of pristine NP, VCE, and the VCEs fully saturated with NP at two wavenumber regions. The VCE polymer gives asymmetric and symmetric  $-\text{CH}_2$  stretchings in the region  $3000\text{--}2800\text{ cm}^{-1}$  [Figure 8(a)], and gives  $-\text{CH}_2-\text{CO}-$  stretching and  $-\text{CO}-\text{O}-$  stretching in the region  $1900\text{--}700\text{ cm}^{-1}$  [Figure 8(b)]. The signature peaks are:

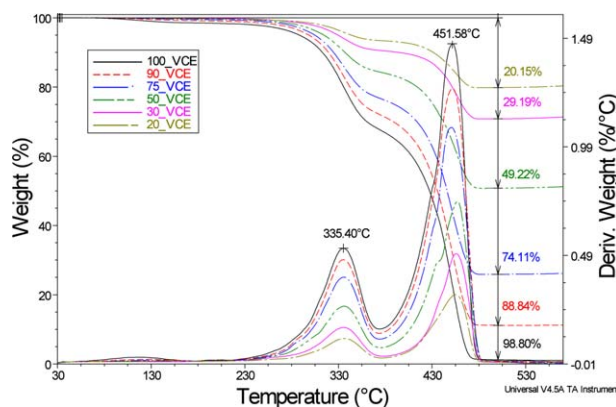


**Figure 5.** Effect of VCE concentration on the DTemps of the VCE polymer. [Color figure can be viewed in the online issue, which is available at [wileyonlinelibrary.com](http://wileyonlinelibrary.com).]

**Table I.** Summary of Weight Loss of VCE and Its Composites at Different Temperature Ranges

Wt loss (%) at different temperature ranges				Cal. Polymer Conc. (%)
RT-240°C	240–380°C	380–500°C	RT-500°C	
0.48	6.16	13.51	20.15	20.39
0.27	9.27	19.57	29.11	29.46
0.60	15.40	33.22	49.22	49.82
0.87	22.96	50.28	74.11	75.01
1.31	27.41	60.12	88.84	89.92
2.05	31.18	65.57	98.80	100.00

$>C=O$  at  $\sim 1740\text{ cm}^{-1}$ , and  $-C-NH-$ ,  $>C=C<$ ,  $-CH_2-$ ,  $-CH_3-$ , and  $>C=CH$  stretching in the aromatic ring at  $1620\text{--}1480\text{ cm}^{-1}$ . These peaks are typically used to identify structural changes in the VCE with aging. For the NP, its signature peaks are  $NO_2$  at  $\sim 1560$  and  $\sim 1320\text{ cm}^{-1}$  and  $-CO-C-C-$  at  $1160\text{--}1040$  and  $870\text{--}840\text{ cm}^{-1}$ . Upon exposure to NP, the FTIR spectra of the samples clearly contain both VCE and NP signature peaks. The interaction between VCE and NP mainly causes two spectral changes: (1) the  $>C=O$  at  $\sim 1740\text{ cm}^{-1}$  becomes slightly broader, and (2) a very broad and weak peak in the  $-NH$  region between  $3600\text{--}3200\text{ cm}^{-1}$  starts to emerge, which are attributed to the H-bonding interaction between VCE and NP. These spectral changes suggest that the interaction between NP and VCE molecules is a physical interaction with no chemical degradation.

Figure 9 shows the FTIR spectra of NP used for the VCE sorption experiments at the various temperatures. The identical spectra of the pristine NP and used NPs (at different temperatures) suggest that no noticeable chemicals leach out of the VCE composites. Furthermore, when the filler particles were exposed to the NP vapor at  $70^\circ\text{C}$  for over a few months, no weight gain was detectable, confirming that the filler does not absorb NP. All of the results confirm that the weight gain of the VCE samples is solely due to the NP uptake by the polymers. With the above study, we conclude that all adsorption experi-

ments were conducted under conditions without detectable chemical degradation in the polymer.

### NP Sorption Study

**Sorption Rate and Solubility of NP.** To determine the sorption equilibrium time, the sorption of NP into the VCE and its composites was studied as a function of contact time. The necessary time to reach the equilibrium depends on the contact area between sorbent (NP) and sorbates (VCE). Figure 10(a) presents the typical profiles of weight gain (NP uptake) in the 100% VCE samples ( $q_t$ ) versus time. The NP uptake is calculated using eq. (1):

$$q_t = \frac{WT_t - WT_i}{WT_i} * 1000 \text{ (mg gram}^{-1}\text{)} \quad (1)$$

$WT_t$ —sample weight at time= $t$ , gram

$WT_i$ —sample weight at time= $0$ , gram

Generally within 500 h the NP weight gain reaches a plateau at the elevated temperatures, which we assume that the NP sorption has reached equilibrium. As temperature increases, the sorption reaches equilibrium within a shorter time and at a higher capacity. The NP saturation in the VCE polymer (also referred to as the NP solubility in the VCE polymer –  $q_e$ ) is  $\sim 340\text{ mg/g}$  at  $22^\circ\text{C}$ . As the temperature increases from  $22$  to  $38^\circ\text{C}$ , the NP solubility increases to  $380\text{ mg/g}$ , which indicates that high temperature favors the NP sorption, and the NP

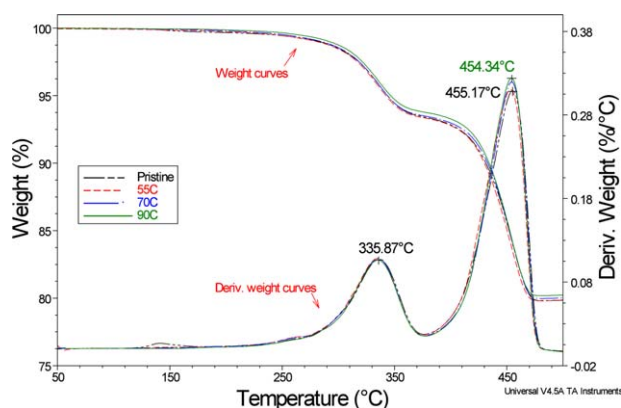


**Figure 6.** Effect of heating temperature on TGA results of the 20% VCE composites after being aged for 6 months under air environment. [Color figure can be viewed in the online issue, which is available at [wileyonlinelibrary.com](http://wileyonlinelibrary.com).]

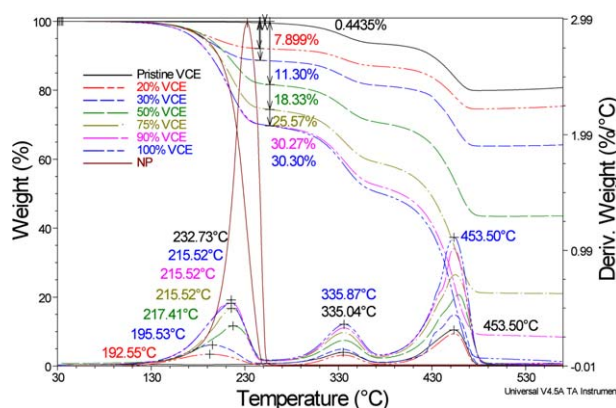


**Figure 7.** Effect of VCE concentration on the decomposition behaviors of NP, VCE, and its composites after being fully saturated with NP at  $70^\circ\text{C}$ . [Color figure can be viewed in the online issue, which is available at [wileyonlinelibrary.com](http://wileyonlinelibrary.com).]



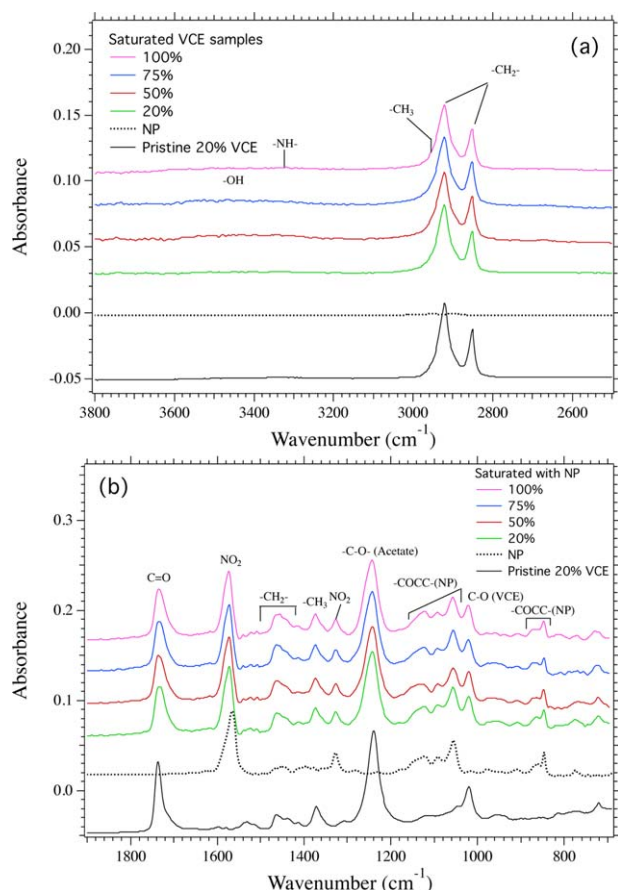


**Figure 8.** FTIR spectra of pristine VCE and VCE/VCE composites fully saturated with NP at 70°C in the regions of 3800–2600 cm<sup>-1</sup> (a) and 1900–700 cm<sup>-1</sup> (b). [Color figure can be viewed in the online issue, which is available at [wileyonlinelibrary.com](http://wileyonlinelibrary.com).]

sorption is endothermic. However, as the temperature further increases from 38 to 70°C, the NP solubility does not increase significantly. The effect of temperature on this value depends on the interaction strength (physical vs. chemical) between sorbent and sorbate molecules.<sup>26</sup> Many factors can contribute to this value. In the earlier studies, some polymers (e.g., ethylene-propylene-diene terpolymer, natural rubber, etc.) were reported to have insignificant changes or even reductions in the equilibrium sorption capacity with increasing temperature. The speculation on this behavior was due to the results of induced crystallinity at higher temperature in the presence of penetrants, which reduces the free energy of mixing.<sup>27</sup> However, when we examined the  $T_g$  of the VCE and VCE composites after the NP exposure at 70°C, their  $T_g$  decreases instead of increase, as shown in Figure 11. The DSC results suggest that the NP uptake does not induce the crystallinity of the VCE polymer, but instead NP allowing the polymer to become more amorphous – presumably increasing the mobility of the polymer chains. One of the possible factors is that high temperature increases the total energy of sorbate molecules, but also increases their escaping tendency, which is typically observed for physical sorption.<sup>26</sup> In fact, a possible mechanism of interaction between VCE and NP molecules is the H-bonding between the —NO<sub>2</sub> groups in

NP and >NH in the VCE; such an interaction could be favored at higher temperatures, but only to a certain extent.

Upon examination the isotherm curve of 100% VCE at ~22°C, the NP sorption gives a two-stage process, as shown in Figure 10(a). The similar behavior of NP adsorption by other types of polymer was reported by Pesce-Rodriguez et al.<sup>28</sup> The authors were not sure whether this was due to the fact that the plasticizer was composed of two molecules, or a reflection of time-dependent boundary condition, or both. Our results suggest that the addition of the filler into the polymer domain significantly impacts the isothermal behavior of the NP sorption. The largest changes are observed for the NP sorption at near room temperature [the red solid lines in Figures 10(b–f)]. As the filler concentration increases from 0 to 80%, the two-stage isotherm process gradually changes to a one-stage process. To understand this impact, we examine the morphological structures of these samples. Figure 12 presents the SEM images of the cross-section of the representative samples of the VCE and five VCE composites. Figure 13 presents the effect of the VCE concentration on the void volumes of the six sample sets, assuming zero void volume in the 100% VCEs. The results suggest that as the filler concentration increases from 0 to 80%, the void volume increases to >15%. Clearly, the filler addition introduces voids in the polymer domain, which in turn increases the interfacial area between particles and polymer allowing NP to easily access the internal portion of the polymer domain, and thus reduces the NP transport resistance. The change in the boundary condition evidently plays an important role in changing the isotherm from a two-stage process into a one-stage process, and impacts the NP sorption process. It is especially true at the low temperature.

Furthermore, the addition of filler not only changes the NP isotherm behavior, but also impacts the apparent NP solubility ( $q_{e,exp}$ ), as seen in Table II. For most VCE composites, their  $q_{e,exp}$  values are larger than those of the 100% VCE at the same temperatures. Again, we believe that the voids in the VCE composites allow NP to accumulate there and result in the higher  $q_{e,exp}$  than that of the pure polymer.

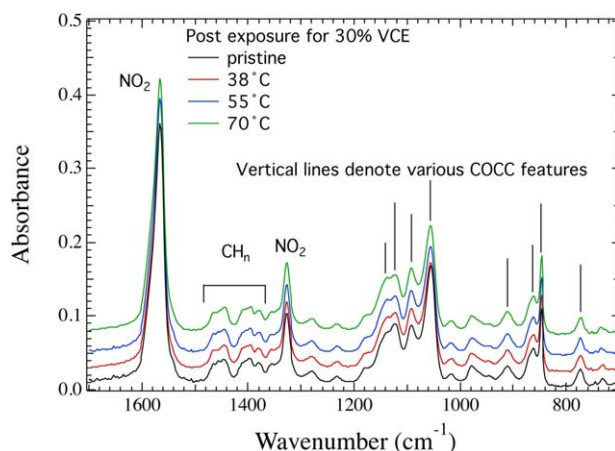


**Figure 9.** FTIR results of liquid NP before and after the 30% VCE immersion experiments at different temperatures. [Color figure can be viewed in the online issue, which is available at [wileyonlinelibrary.com](http://wileyonlinelibrary.com).]

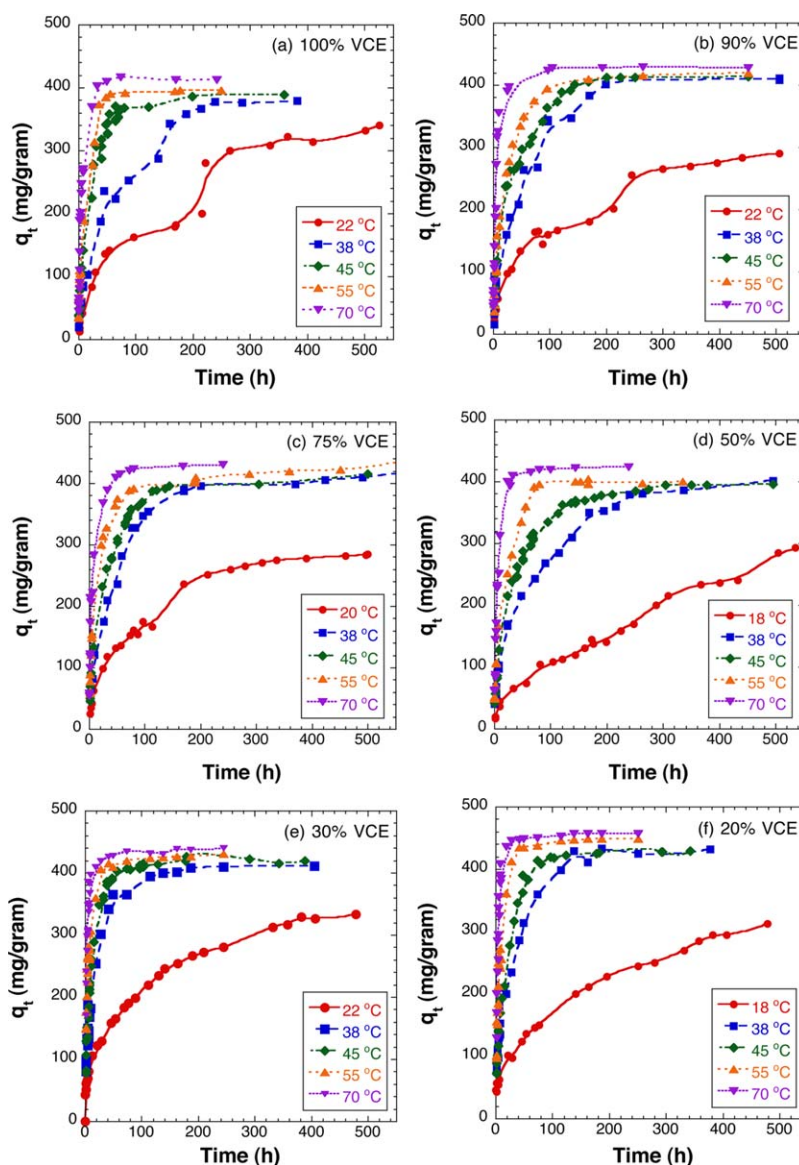


**Figure 10.** Effect of temperature on the NP sorption into the VCE polymer (a) and the VCE composites (b–f). (Note: the ambient temperature varies from time to time;  $q_t$  = NP weight/VCE weight (mg/gram), average data are used for all data points). [Color figure can be viewed in the online issue, which is available at [wileyonlinelibrary.com](http://wileyonlinelibrary.com).]

It is worth noting that the NP isotherms of the VCE polymer and VCE composites at ambient temperature are noticeably different from these obtained at the elevated temperature. The DSC data suggests that the vinyl-acetate component of the polymer typically softens and melts above 37°C.<sup>29</sup> The VCE terpolymer, contains ~43% of this group. The softening/melting of the vinyl-acetate group in VCE can improve the mobility of the polymer chains leading to an increase in the free volume. At the same time, increased temperature significantly decreases the viscosity of NP (see Figure 14). Compared with the room temperature, these two factors allow the NP molecules to permeate into the deep portion of the polymer domain with much lower resistance, and thus increase diffusion process of NP. These thermally induced changes in the physical properties of both VCE and NP may explain the large difference between the data col-

lected from 18 to 22°C and the data from above 37°C. Therefore, bearing this in mind, in the following discussion, we separate the 18–22°C data from the data collected from the higher temperatures.

**NP Sorption Mechanism.** Sorption kinetics is one of the most common experimental techniques to study the diffusion of small molecules in polymers. When the small molecules transport in a rubbery polymer well above their glass transition temperature and the boundary condition is rapidly established, the transport is diffusion controlled and can be described using ideal Fickian diffusion,<sup>30,31</sup> as expressed in the Fick's second law:

$$\frac{\partial C(x,t)}{\partial t} = D \frac{\partial^2 C}{\partial x^2} \quad (2)$$

where  $C(x,t)$  is the concentration at position  $x$  at time  $t$  and  $D$  is the diffusion coefficient.

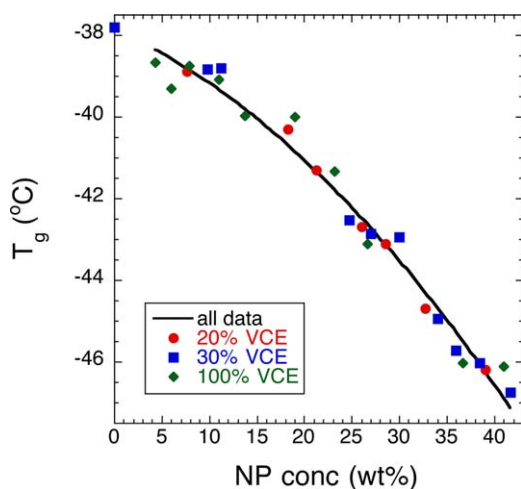


**Figure 11.** Effect of the NP uptake on the  $T_g$  of the VCE and its composites exposed to NP at 70°C for different times (NP conc. is normalized to the VCE concentration in the samples). [Color figure can be viewed in the online issue, which is available at [wileyonlinelibrary.com](http://wileyonlinelibrary.com).]

In 1975, Crank developed a well-known solution which is suitable to moderate and long time approximation.<sup>32</sup> In this technique, a polymer film of thickness  $2l$  is immersed into the infinite bath of penetrant, then concentrations,  $C(t)$ , at any spot within the film at time  $t$  is given by eq. (3)<sup>33,34</sup>:

$$\frac{C_t}{C_\infty} = 1 - \frac{4}{\pi} \sum_{n=0}^{\infty} \frac{(-1)^n}{2n+1} \exp\left[\frac{-D(2n+1)^2 \pi^2 t}{4l^2}\right] * \cos\left[\frac{(2n+1)\pi x}{2l}\right] \quad (3)$$

where  $C_\infty$  is the amount of accumulated penetrant at equilibrium, i.e. the saturation equilibrium concentration within the

system.  $2l$  is the distance between two boundaries layers. Integrating eq. (3) yields eq. (4)—giving the mass of the sorbed penetrant by the film as a function of time  $t$ ,  $q_t$ , and compared with the equilibrium mass,  $q_e$ .

$$\frac{q_t}{q_e} = 1 - \sum_{n=0}^{\infty} \frac{8}{(2n+1)^2 \pi^2} \exp\left[\frac{-D(2n+1)^2 \pi^2 t}{4l^2}\right] \quad (4)$$

Using the following minimization method, the experimental data were fit by using eq. (4) and adjusting the diffusion coefficient  $D$  to minimize the error of the dimensionless mean square root ( $\gamma$ ) given by

$$\gamma = \left[ \frac{1}{N} \sum_{i=1}^N \frac{[q_i^T - q_i]^2}{q_e^2} \right]^{1/2} \quad (5)$$

where  $N$  is the number of experimental data points and  $q_i^T$  is the calculated average weight at time  $t_i$ . The smaller the dimensionless mean square root error is, the better the theoretical fit is. The plots of  $q_t$  vs  $t^{1/2}$  for the 100% VCE and 20% VCE composites are given in Figure 15(a,b), respectively. The lines are the calculated results of fitting the data as two-side diffusion into a thin film with different diffusion coefficients at different temperatures for the different sample sets. The calculated diffusion coefficients and the values of the dimensionless mean square root error are summarized in Table II. There is a  $\pm 0.2 \times 10^{-9} \text{ cm}^2 \text{ s}^{-1}$  uncertainty for all calculated diffusion coefficients. This uncertainty was estimated from the deviations of the best-fit  $D$  coefficients of the individual experiments from the overall best-fit single  $D$  for each temperature set. Clearly, the  $q_t$  vs  $t^{1/2}$  plots for the room temperature experiments are different from the ones obtained at the elevated temperatures, which is due to the different physical properties of both VCE polymer and NP

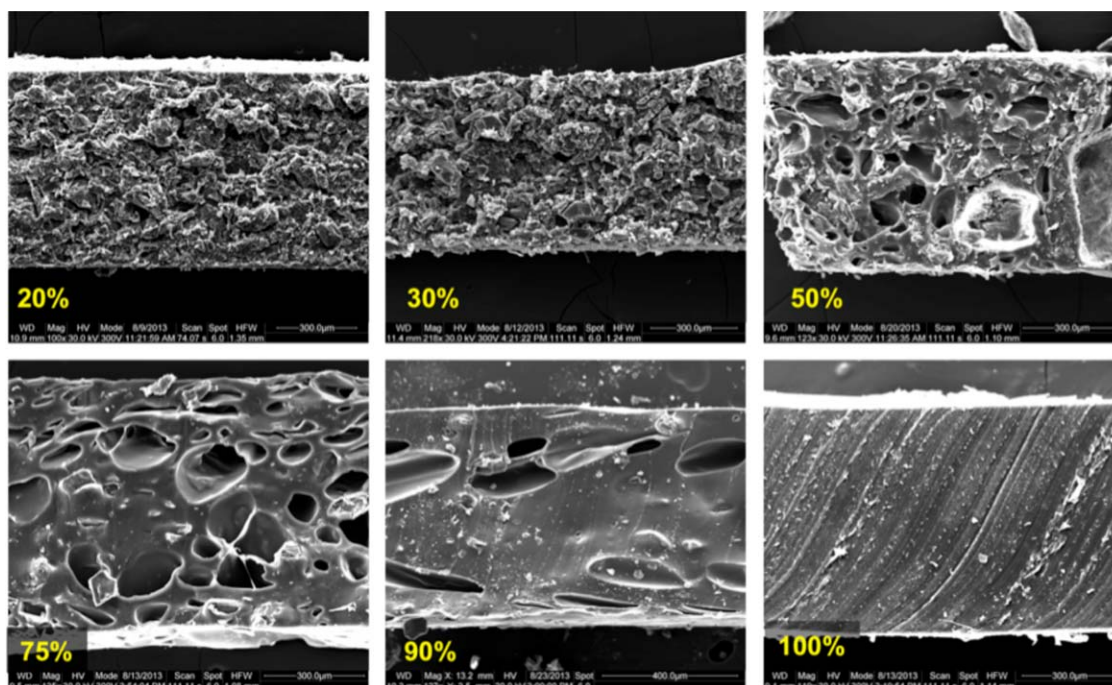


**Figure 12.** SEM images of the cross-section of the VCE and its composites. [Color figure can be viewed in the online issue, which is available at [wileyonlinelibrary.com](http://wileyonlinelibrary.com).]



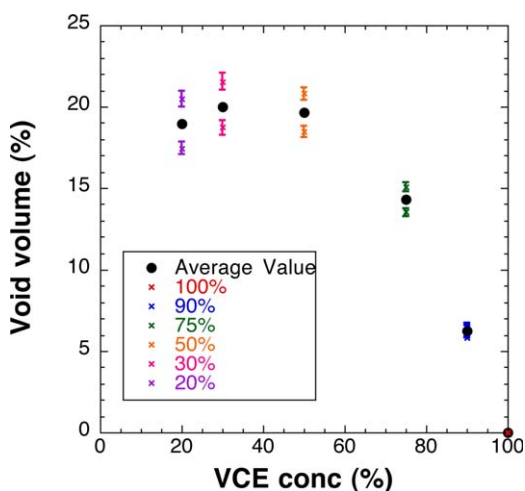


**Figure 13.** Effect of VCE concentration on the void volume of the VCE composites (assuming that 100% VCE is completely dense). [Color figure can be viewed in the online issue, which is available at [wileyonlinelibrary.com](http://wileyonlinelibrary.com).]

liquid at the different temperature ranges. The experimental data are scattered along the line for the 100% VCE samples at 18°C, which gives the largest calculated error (0.0641). As the temperature and filler concentration increase, the isotherms of NP in the VCE and VCE composites show similar curvature on a multi-time scale with much better fits. This phenomenon is commonly observed for the molecular diffusion in polymeric systems<sup>21,22,27,31,35,36</sup> in the cases like this with no significant swelling at the early stage of sorption and the experiments are conducted above the  $T_g$  of polymer.<sup>15,19,21,27,31</sup> Our data agree with the literature. All of the curves show initially a linear increase up to >50% of the equilibrium concentration and exponential behavior in long time ranges, which indicates that the diffusion is Fickian within an experimental error.

As the temperature increases from 22 to 70°C, the diffusion coefficients of NP in the 100% VCE increase from 0.88 to  $18.51 \times 10^{-9} \text{ cm}^2 \text{ s}^{-1}$  in the VCE polymer. The increased diffusion coefficients can be explained that as the temperature increases, in addition to the increased mobility of NP molecules, the amplitude of segmental oscillations of the polymer chains also increases. Greater segmental motion results in an increase in the size of free volume and subsequent increases in diffusivity of NP inside the polymer domain.<sup>19,27,36</sup> The temperature effect applies to the polymer chains regardless of the presence of fillers. Therefore, for the six sample sets, their diffusion coefficients increase with increasing temperature.

On the other hand, the effects of the filler concentration are not straightforward. As the SEM images suggest, the large variation in the size and shape of voids present in the filler and polymer domain results in complicated morphologies with different voids, void distribution, and interfacial area between the polymer and fillers. Therefore, the NP transport in the VCE composites—a heterogeneous medium is greatly complicated by the morphological structures. To estimate the diffusivity of NP in the VCE composites, we used the most common approach which assumes that the transport in the polymer domain within

a composite is analogous to transport in a homogeneous sample of the phase at the same conditions (e.g., temperature and concentration).<sup>21</sup> Using this analogous approach requires one valid assumption that the transport along the phase boundaries is insignificant and the size of the sorbent molecules is much less compared with the size of the phase domains. Although the SEM images suggest that the sizes of polymer domain (>10  $\mu\text{m}$ ) are much larger than the NP molecular size, the effect of the phase boundary in the highly filled VCE composites may be significant. On close examination of the plots in Figure 15(b), one notices that the data points at short time are above the lines for the low temperature sets. The same observation is obtained for the 30% VCE composites as well, which suggests that these initial  $q_t$  vs.  $t^{1/2}$  lines do not pass through the origin, and departure from the ideal Fickian behavior. This deviation may be due to the effect of the phase boundary in these composites. As the filler concentration substantially increases, the heterogeneity significantly increases. The large amount of voids enhance the phase boundary transport of NP and enable NP molecules to quickly accumulate at the interfaces before the diffusion into the polymer domain really starts, which may explain the off-set in their  $q_t$  vs.  $t^{1/2}$  plots. However, as temperature increases, this nonideal behavior diminishes, owing to the large increase in the mobility of the polymer chains and NP molecules. The great increases in the diffusion coefficients are obtained at 70°C in which the effect of interfacial boundary transport becomes less important. Furthermore, at the high temperature, the gravimetric measurement is not sensitive enough to detect this boundary effect and the diffusion dominates the NP sorption process.

Essentially, the addition of fillers into the VCE domain brings two counter effects: (1) creates voids in the polymer domain, which increases the interfacial area and thus reduces the transport resistances of NP diffusion, and (2) creates the obstacle in the pathway of the NP diffusion. These two counter effects result in a nonmonotonic impact on the NP transport in the VCE composites. Therefore, no clear trend is found from the effect of the filler concentration on the NP diffusivity in the VCE composites for a given temperature. Among the five VCE composites, the smallest diffusivities are obtained for the 50% VCE composites. On the contrary, the largest diffusion coefficients are obtained for the 30% VCE composites. Although the void volumes of these two sets are similar to one another, the SEM images suggest that the void sizes in the former are large but isolated, whereas the void sizes in the latter are much smaller, but well distributed in the polymer matrix. Therefore, for the 50% VCE composites, the second effect dominates and slows down the NP diffusion. On the contrary, for the 30% VCE composites, the first effect dominates and enhances the NP diffusion.

Clearly, NP transport through the VCE domain occurs by a solution-diffusion mechanism. The mass transfer in many rubbery polymers, like VCE here, is achieved by the combination of solubility and diffusivity of liquid solvents. In this case, the permeability is commonly used to describe the mass transfer phenomenon. It is a product of the effective diffusivity and solubility of NP. The calculated values are also given in Table II.



**Table II.** Summary of  $q_{e,exp}$  Diffusion Coefficient ( $D$ ), Error of Dimensionless Mean Square Root ( $\gamma$ ), and Permeability ( $P$ ) of NP Sorption in VCE and VCE Composites at Different Temperatures

VCE conc. (%)	Temperature (K)	$q_{e,exp}$ (mg g <sup>-1</sup> )	$D/10^{-9}$ (cm <sup>2</sup> /s)	$\gamma$	$P(=DS)/10^{-9}$ (cm <sup>2</sup> /s)
100	295	340.1	0.88	0.0641	0.30
	311	379.7	1.85	0.0366	0.70
	318	389.0	5.51	0.0273	2.14
	328	395.9	8.17	0.0311	3.24
	343	417.2	18.51	0.0373	7.66
90	295	290.4	1.42	0.0492	0.41
	311	408.1	2.96	0.0601	1.21
	318	414.0	4.66	0.0331	1.93
	328	418.0	7.04	0.0235	2.92
	343	430.1	25.66	0.0504	10.98
75	295	284.4	1.76	0.0313	0.50
	311	410.1	3.51	0.0224	1.40
	318	415.0	4.96	0.0162	2.01
	328	422.0	9.90	0.0275	4.11
	343	430.0	24.44	0.0547	10.46
50	291	298.8	0.75	0.0638	0.22
	311	398.2	2.77	0.0332	1.10
	318	402.4	4.72	0.0290	1.90
	328	405.0	9.41	0.0275	3.81
	343	425.0	26.35	0.0216	11.20
30	295	333.3	0.98	0.0493	0.33
	311	411.5	5.14	0.0416	2.12
	318	422.7	7.09	0.0321	3.00
	328	428.0	15.63	0.0541	6.69
	343	438.0	31.03	0.0502	13.59
20	291	312.5	0.94	0.0508	0.29
	311	425.0	4.37	0.0471	1.85
	318	432.8	5.51	0.0248	2.36
	328	449.0	13.46	0.0293	6.04
	343	456.5	31.25	0.0369	14.27

Here the values of solubility are taken as gram of NP sorbed per gram of the VCE polymer. Since both solubility and diffusivity of NP increase with increasing temperature, the permeability increases with temperature as well.

#### Thermodynamics of the NP Sorption into VCE and VCE Composites

To calculate the thermodynamic parameters at an equilibrium state, such as the heat of sorption ( $\Delta H_S$ ), the Van't Hoff equation ( $S = S_0 \exp(-\Delta H_S/RT)$ ) was applied using solubility values ( $q_{exp}$ ) obtained from the isothermal experiments. The calculated  $\Delta H_S$  values are summarized in Table III. The positive val-

ues confirm the endothermic characteristic of the NP sorption, which involves the Henry's law and requires both the formation of a sorption site and the dissolution of the species into that site. At the same time, the sorption process is governed by the Langmuir type sorption (hole filling). With the Langmuir mode, the site already exists in the polymer domain, by hole filling, yields more exothermic heat of sorption. These two mechanisms compensate each other, which result in a small heat of sorption for the NP sorption process. The positive heat of sorption also suggests that the polymer-polymer interaction and the NP-NP interaction have less enthalpy than the polymer-NP interaction. Without external energy, the NP-NP

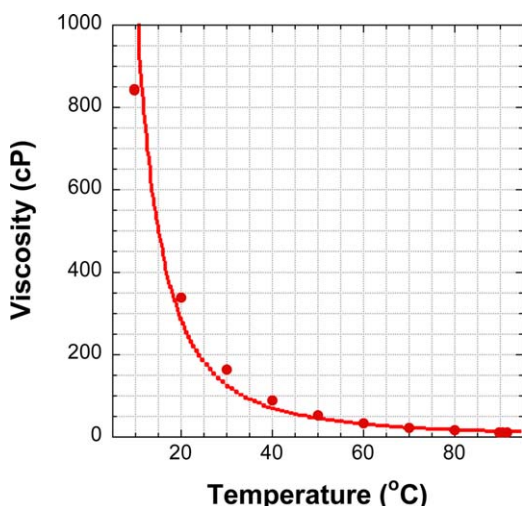


**Figure 14.** Effect of temperature on the liquid NP viscosity (Brookfield-III viscometer was used for the measurement). [Color figure can be viewed in the online issue, which is available at [wileyonlinelibrary.com](http://wileyonlinelibrary.com).]

interactions are more favorable than the interaction between NP and VCE molecules. Therefore, the NP sorption is mainly due to NP diffusion into the polymer domain driven by the NP concentration gradient built at the boundary layer, but not much due to the physical attribution of VCE.

The Arrhenius equation for calculating adsorption activation energy is expressed as:

$$D = A_D \exp\left(-\frac{E_{aD}}{RT}\right) \quad (6)$$

where  $A_D$  is the pre-exponential factor,  $E_a$  the activation energy of diffusion ( $\text{kJ mol}^{-1}$ ),  $R$  the universal gas constant ( $8.314 \text{ J mol}^{-1} \text{ K}^{-1}$ ) and  $T$  the temperature ( $\text{K}$ ). This activation energy will be greater with the stronger polymer inter- and intra-chain interactions, and the greater rigidity of the chains.<sup>27</sup> We used this equation to fit the diffusivity versus temperature. Due to the phase change occurring between room temperature and  $38^\circ\text{C}$ , we did not include the room temperature data in this calculation. The determined activation energies are summarized in Table III. The activation energy of NP diffusion into the VCE polymer was  $\sim 59.2 \pm 1.5 \text{ kJ mol}^{-1}$ . The uncertainty in these values was due to the uncertainty of the diffusivities. Together with Van der Waals forces and electrostatic attractions, the interactions among inter- and intra-chains in the VCE polymer are due to the affinity between the carbonyl oxygen group ( $>\text{C}=\text{O}$ ) at both ester and urethane links and the secondary amine group ( $>\text{NH}$ ) in the urethane links. Similarly, there are some interactions among NP molecules. This energy is required to create an opening between polymer chains large enough to allow the NP molecules to pass. Therefore,  $E_{aD}$  here is a function of the inter- and intra-chain interactions that NP molecules must be able to overcome in order to create the space for a unit diffusional jump. This energy is equivalent to 3–4 H-bonds based on the assumption of the average  $\text{O}:\text{--HN-}$  and  $\text{O}:\text{--HO-}$  hydrogen-bonding energy between 8 and  $21 \text{ kJ mol}^{-1}$ .<sup>37</sup> This value is in the range similar to that of nitro-plasticizers in a

rubbery polymer.<sup>11,38</sup> The permeability can also be expressed in terms of an Arrhenius-type relationship. The estimated Arrhenius quantities are summarized in Table III. The difference between  $E_a^P$  and  $E_a^D$  should be equal to the heat of sorption.

As the filler concentration increases, the activation energy of NP diffusion varies. In producing the VCE composites, the filler addition introduces voids in the polymer domains, which presumably creates more surface area, interfacial boundary, and acts as high diffusivity paths. However, depending on the void size, void distribution, the connectivity among the voids, and the interfacial area between the filler and polymer, the accessibility of these voids varies significantly from sample to sample. Therefore, the two counter effects due to the filler addition result in the non-monotonic impact in the activation energy as well. For the 30% VCEs, the increased interfacial area definitely brings a productive effect and reduces the activation energy of the NP diffusion process. On the contrary, for the 50% VCE composites, because of the poor accessibility of their voids and/or the

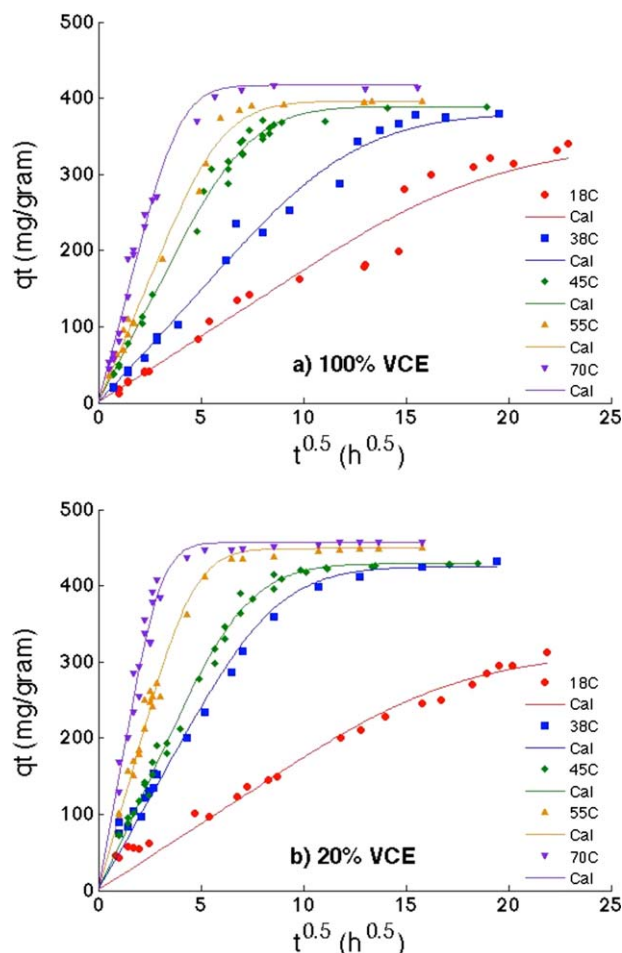


**Figure 15.** The weight gain of the VCE samples versus the square root of time ( $t^{1/2}$ ) (NP sorption into 100% VCE (a) and 20% VCE composite (b)). The data points are experimental values. The lines are the fit by using Fickian diffusion model. [Color figure can be viewed in the online issue, which is available at [wileyonlinelibrary.com](http://wileyonlinelibrary.com).]

**Table III.** Summary of Heat of Sorption and Activation Energies of NP Sorption into VCE and VCE Composites

VCE conc. (wt %)	$\Delta H_S^a$ (kJ mol <sup>-1</sup> )	$E_a^{Db}$ (kJ mol <sup>-1</sup> )	$E_a^{Pb}$ (kJ mol <sup>-1</sup> )
100	2.24	59.2	61.7
90	1.50	58.7	59.9
75	1.32	54.5	56.8
50	1.69	62.3	64.1
30	1.65	51.5	53.1
20	2.05	57.3	59.4

<sup>a</sup> Calculated from the values of  $q_{e,exp}$  using Van's Hoff equation.

<sup>b</sup> Calculated from the diffusion coefficient ( $D$ ) or permeability ( $P$ ) using eq. (6).

large obstacle of the filler to NP diffusion, the activation energy of the NP diffusion increases noticeably.

## CONCLUSIONS

It is well known that the organic molecule diffusion into the polymer domain is an important but a complicated subject.<sup>19–22,30,36</sup> With a phase change, diffusion coupled with NP sorption at the elevated temperatures, and the morphological changes from homogeneous to heterogeneous in the polymer domain, we understand that we are tackling a very complicated problem. Furthermore, the transport process of the NP migration in the application systems is far more complicated than the NP sorption conducted here because the NP concentration at the surface of the VCE composite changes with the exposure conditions (time, temperature, compression, etc). Here, we studied the NP sorption by the conventional gravimetric method with the constant concentration at the polymer boundary and used the simplest model to analyze the experimental results, and hope to provide some insight into the dependence of the polymer structures on the variation in the NP uptake at different temperatures and filler concentrations. Although the polymer relaxation often occurs concurrently with the sorption process, this study was conducted away above the  $T_g$  of the VCE polymer, and the experimental time scale is much less than the VCE relaxation rate. Therefore, the classical Fickian model describes the NP sorption process well. Increased temperature increases the mobility of the polymer and thus increases the free volume in the polymer domain. Simultaneously, increased temperature also largely reduces the viscosity of the NP and in turn increases its mobility. Therefore, temperature accelerates NP diffusion and hence NP sorption. However, for the VCE composites, as the filler concentration increases, the polymer domain changes from homogeneous into heterogeneous phase. The large variation in the sizes and shapes present in the filler and polymer domain results in complicated morphologies. Therefore, the addition of the filler brings two counter effects, which result in a nonmonotonic effect on both NP sorption and diffusion processes as the filler concentration increases. To fundamentally understand the effects of the NP concentration variation, the morphology, and the phase changes in the polymer domains on the NP mass transport

process, a more systematic study should be conducted to consider these factors with better control of the filler sizes and the filler/void distributions, and with more temperature intervals along the temperature range.

## ACKNOWLEDGMENTS

The authors thank Stephen Birdsell for fruitful discussions. They thank John Barton, Tom Robison and Matt Trimmer (KCP) for helping on the VCE material production. Viscosity measurements were conducted by Manuel Chavez, for which the authors are thankful. This work is funded by Enhanced surveillance campaign 8 by the US Department of Energy's National Nuclear Security Administration under contract DE-AC52-06NA25396.

## REFERENCES

- Labouriau, A.; Densmore, C.; Meadows, K.; Cordova, B.; Lewis, R. LANL Internal Report, LA-UR-06-5294, Los Alamos, NM, **2006**, p 17.
- Densmore, C.; Eastwood, E. LANL Internal Report, LA-UR-06-6812, Los Alamos, NM, **2006**, p 52.
- Letant, S. E.; Wilson, T. S.; Alviso, C. T., IV, W. S.; Heather, A. M.; Pearson, M.; Herberg, J. L.; Chinn, S. C.; Maxwell, R. S. LLNL Internal Report, Livermore, CA: **2011**, p 27.
- Wilson, P. M. KCP Internal Report, Kansas City, MO: **1997**, p 17.
- Wilson, P. M. KCP Internal Report, Kansas City, MO: **1998**, p 51.
- Yang, D.; Tornga, S.; Hubbard, K.; Labouriau, A.; Birdsell, S. A. LAUR-2011-03582, Present in JOWOG 28 Main Meeting, Y-12 National Security Complex, Knoxville, TN, June **2011**, p 26.
- Yang, D.; Pacheco, R.; Henderson, K.; Hubbard, K.; Brian Patterson; Devlin, D.; Welch, C.; Kelly, D. LA-CP-13-0121, Presented in JOWOG 28 Main Meeting, Aldermaston, UK, September **2013**, p 20.
- Kumari, D.; Balakshie, R.; Banerjee, S.; Singh, H. *Rev. J. Chem.* **2012**, 2, 26.
- Polymer-bonded explosive, from Wikipedia, the Free encyclopedia, on Oct. 27, **2013**.
- Rauch, R. B.; Behrens, R. *Propellants, Explosives, Pyrotechnics* **2007**, 32, 20.
- Provatas, A. Aeronautical and Maritime Research Laboratory Internal Report, DSTO-TR-0996, Australia, April **2000**.
- Salazar, M. R.; Kress, J. D.; Lightfoot, J. M.; Russell, B. G.; Rodin, W. A.; Woods, L. *Propellants, Explosives, Pyrotechnics* **2007**, 33, 182.
- Salazar, M. R.; Thompson, S. L. E.; Laintz, K.; Meyer, T. O.; Pack, R. T. *J. Appl. Polym. Sci.* **2007**, 105, 1063.
- Kress, J. D.; Wroblewski, D. A.; Langlois, D. A.; Orler, E. B.; Lightfoot, J. M.; Rodin, W. A.; Huddleston, C. O.; Woods, L.; Russell, B. G.; Salazar, M. R.; Pauler, D. K. In *Polymer Degradation and Performance*; Celina, M. C.; Wiggins, J. S.; Billingham, N. C., Eds.; American Chemical Society: Washington, DC, **2008**, p 12.



15. Gottlieb, L.; Bar, S. *Propellants, Explosives, Pyrotechnics* **2003**, 28, 6.
16. Fletcher, M.; Powell, S. LANL Internal Communication, Los Alamos, NM, **2003**, p 10.
17. Spontarelli, T. 21st Aging, Compatibility and Stockpile Stewardship Conference, Albuquerque, Sept. 30 - Oct. 2, **1997**, p 2.
18. Fletcher, M.; Powell, S. LANL Internal Report, LAUR-02-1287, **2002**, p 6.
19. Vesely, D. *Int. Mater. Rev.* **2008**, 53, 17.
20. Ju, S. T.; Duda, J. L. *Ind. Eng. Chem. Res. Dev.* **1981**, 20, 6.
21. Duda, J. L. *Pure Appl. Chem.* **1985**, 57, 10.
22. Vermeulen, T. *Ind. Eng. Chem.* **1953**, 45, 13.
23. Finger, M. Lawrence Livermore Laboratory, Livermore Internal report, **1972**, p 16.
24. Rindone, R.; Donald A. Geiss, J.; Miyoshi, H. IM/EM Technology Implementation in the 21st century, Hyatt Regency San Antonio, Texas, Nov. 27-30, **2000**.
25. Smith, R. M.; Baker, G. K.; Smith, C. H. In *Chemistry and Properties of Crosslinked Polymers*; Labana, S. S., Ed.; Academic Press, Elsevier: New York, **1977**.
26. Ho, Y. S.; McKay, G. *ITrans IChemE* **1998**, 76, 9.
27. Harogopad, S. B.; Aminabhavi, T. M. *Macromolecules* **1991**, 24, 8.
28. Pesce-Rodriguez, R. A.; Mieser, C. S.; McNesby, K. L.; Fifer, R. A.; Kessel, S.; Strauss, B. D. *Appl. Spectroscopy* **1992**, 46, 6.
29. Perez, E.; Lujan, M.; Salazar, J. M. D. *Macromol. Chem. Phys.* **2000**, 201, 6.
30. Joshi, S.; Astarita, G. *Polymer* **1978**, 20, 4.
31. Ottino, J. M.; Shah, N. *Polym. Eng. Sci.* **1984**, 24, 10.
32. Crank, J. *The Mathematics of Diffusion*; Oxford University Press: New York, **1975**.
33. Comyn, J. *Polymer Permeability*; Chapman & Hall: London, **1985**.
34. Karimi, M.; Markora, J. e-book entitled *Mass Transfer in Chemical Engineering Processes*; Jozef, M., Ed.; InTech: Shanghai, **2011**.
35. Cheung, W. H.; Szeto, Y. S.; McKay, G. *Bioresource Technol.* **2007**, 98, 8.
36. Jenkins, R. B.; Park, G. S. *J. Membr. Sci.* **1983**, 15, 13.
37. Hydrogen bond from Wikipedia - The Free Encyclopaedia; on Nov. 29, **2013**.
38. Provatas, A. *Energetic Mater.* **2003**, 21, 9.